Communications

DOI: 10.1002/anie.200502007

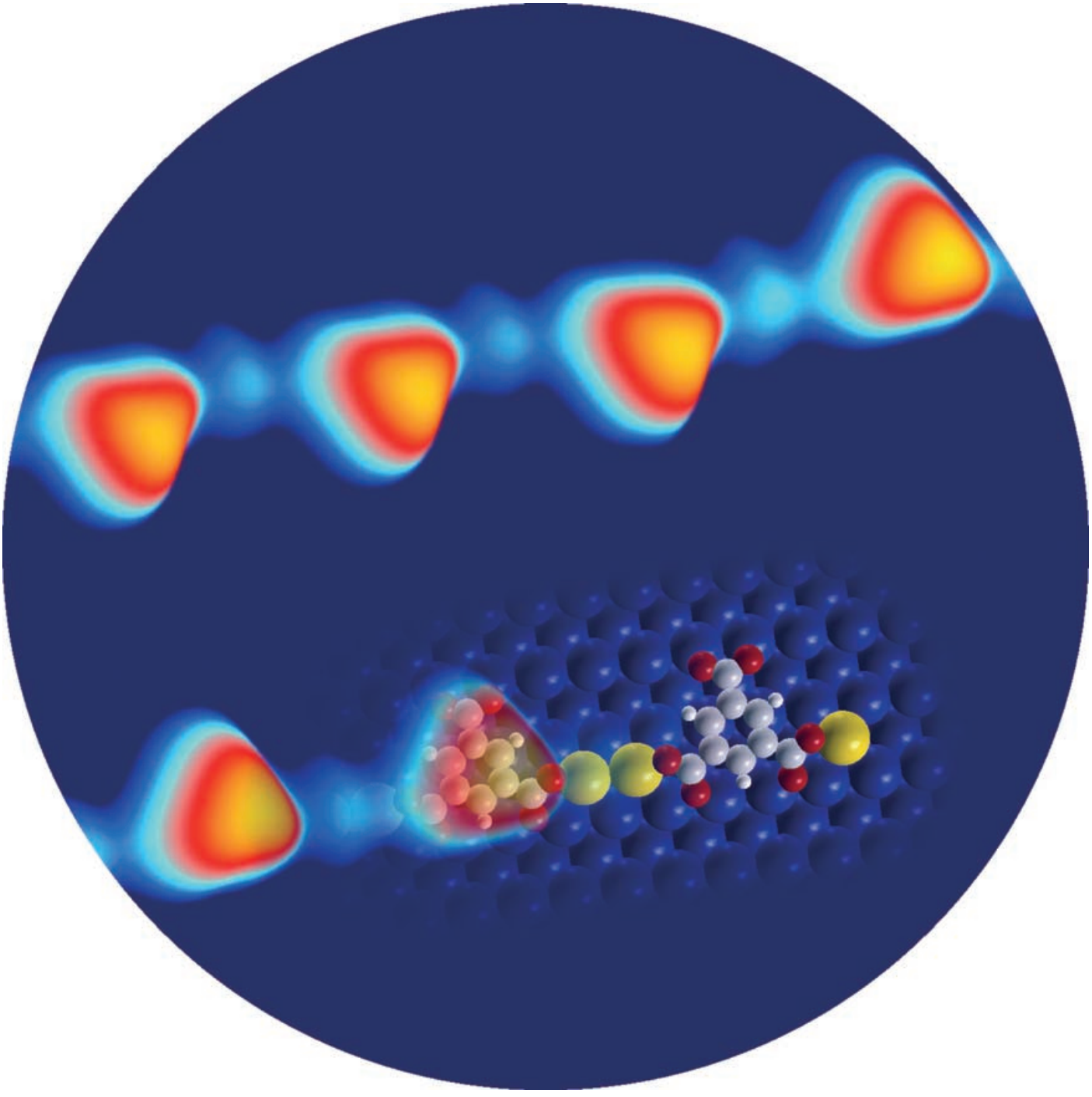

Highly anisotropic metal surfaces can drive the formation of metal–organic coordination chains, as shown by scanning tunneling microscopy analysis and density functional calculations. For details about the templated coordination of Cu and Fe atoms with trimesitylic acid on a Cu(110) surface, see the Communication by T. Classen, S. Fabris, K. Kern, and co-workers on the following pages.

Coordination Chains

DOI: 10.1002/anie.200502007

Templated Growth of Metal–Organic Coordination Chains at Surfaces**

Thomas Classen, Guido Fratesi, Giovanni Costantini, Stefano Fabris,* Frank Louis Stadler, Cheolkyu Kim, Stefano de Gironcoli, Stefano Baroni, and Klaus Kern**

Metal–organic coordination networks (MOCNs) formed by coordination bonding between metallic centers and organic ligands can be efficiently engineered to exhibit specific magnetic, electronic, or catalytic properties.[1–6] Instead of depositing prefabricated MOCNs onto surfaces, it has been recently shown that two-dimensional (2D) MOCNs can be directly grown at metal surfaces under ultrahigh vacuum (UHV), thus creating highly regular 2D networks of metal atoms.[7–12] These grids have been pointed out to be potentially relevant for devices that involve sensing, switching, and information storage.[13,14] We show here that this approach offers the additional advantage to predefine the geometry of the MOCN by using the substrate as a template to direct the formation of novel 1D metal–organic coordination chains (MOCCs).

The templating role of substrates is well known in the field of surface epitaxial growth.[15–19] Among the highly anisotropic substrates, the Cu(110) surface is one of the most commonly used (Figure 1a and b). To demonstrate its strong 1D templating effect on organic molecules, a ligand with a triangular symmetry was selected, namely 1,3,5-benzenetricarboxylic acid (trimesic acid, TMA; Figure 1c). The three-fold rotation symmetry of TMA supports the formation of hexagonal 2D and 3D architectures,[20–22] therefore strongly disfavoring the linear geometry. On the isotropic Cu(100) surface, TMA forms 0D carboxylate complexes and 2D networks.[9,10]

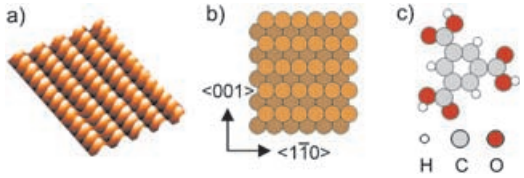

Figure 1. a) High-resolution STM image in 3D representation and b) structural model of the Cu(110) surface. c) Trimesic acid (TMA).

The deposition of TMA on Cu(110) under UHV at 300 K results in the formation of 1D chains along the $\langle 1\bar{1}0\rangle$ direction, as observed by scanning tunneling microscopy (STM). This deposition temperature is high enough to provide mobile Cu adatoms through evaporation from kinks and steps onto the terraces.[23] Analysis of similar systems by X-ray photoelectron spectroscopy[24,25] showed that these adatoms catalyze the deprotonation of molecular carboxylate groups. The adatoms are furthermore necessary for the formation of copper carboxylate complexes.[23,24,26] Deposition at lower temperatures, 210 K and 250 K, resulted in disordered structures with a tip-to-tip bonding motif. This signature, which is never observed above 300 K, is characteristic for intermolecular dimeric hydrogen bonds of carboxylate groups,[20–22,24] thus indicating that the carboxylate groups are protonated at temperatures below 300 K. Upon annealing to 300 K, these structures yield to the same 1D chains described above. The chains formed at 300 K typically show irregular kinks and poor long-range order. These inhomogeneities are removed by post-annealing to 380–410 K to yield straight and highly periodic chains, referred to as MOCC-I hereafter (Figure 2). At low coverage, chains predominantly attach to step edges, whereas upon increasing the coverage chain nucleation takes place also on terraces.

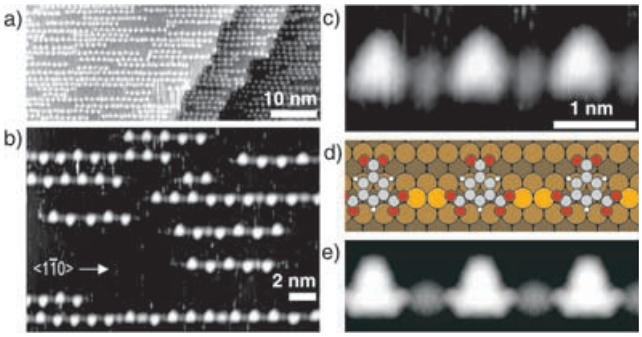

Figure 2. Representative STM images of [-Cu-TMA-Cu-]$_n$ chains (MOCC-I) on Cu(110) for TMA coverages of a) 0.36 and b) 0.13 monolayers (ML), respectively. Comparison of c) the high-resolution STM image of MOCC-I, d) the atomistic MOCC-I model, and e) the corresponding simulated STM image.

These findings allow the substrate templating effect to be rationalized as follows: Upon deprotonation, the molecule–molecule interaction (favoring hexagonal geometries) is overcome by the molecule–substrate interaction, which effectively controls the 1D character of these MOCCs.

The chains consist of triangles alternating with round protrusions (Figure 2b and c). The apparent height of the two units is significantly different, 140 ± 30 pm and 75 ± 20 pm, respectively, when scanning at -1 V and 1 nA. Following previous analysis,[9,10,20–22] the triangles are identified as flat-lying TMA molecules. The round protrusions can be attrib-

[*] T. Classen, Dr. G. Costantini, Dr. F. L. Stadler, Dr. C. Kim, Prof. K. Kern
Max-Planck-Institut für Festkörperforschung
Heisenbergstr. 1, 70569 Stuttgart (Germany)
Fax: (+49) 711-689-1662
E-mail: t.classen@fkf.mpg.de
k.kern@fkf.mpg.de
G. Fratesi, Dr. S. Fabris, Prof. S. de Gironcoli, Prof. S. Baroni
SISSA and INFM-CNR DEMOCRITOS National Simulation Center
Via Beirut 2–4, 34014 Trieste (Italy)
Fax: (+39) 040-3787-528
E-mail: fabris@democritos.it

[**] The authors wish to acknowledge Nian Lin, Magalí Lingenfelder, Alexander Schneider, and Giacinto Scoles for fruitful discussions, as well as HPC-EUROPA (project #506079) and INFM Progetto Calcolo Parallelo for computer resources.

uted to Cu adatoms,[7,9,10] coordinated by two of the carboxylate groups of the TMA molecule. The third functional group of TMA is pointing out of the chain with no preferential up or down orientation (Figure 2b).

The periodicity of MOCC-I along $\langle 1\bar{1}0\rangle$ is five Cu lattice spacings (12.70 ± 0.15 Å). High-resolution STM images indicate that the distance between the Cu protrusions and the oxygen atom of the molecular carboxylate groups is approximately 2.8 Å, a rather large value when compared to the typical Cu–O bond length of 1.9–2.2 Å.[27] The simplest [-TMA-Cu-]$_n$ chain model for the adsorption geometry of MOCC-I seems therefore to be outruled by these observations.

Indeed, the lowest energy structure of MOCC-I as predicted by density functional theory (DFT) calculations is a [-Cu-TMA-Cu-]$_n$ chain in which a dimer of Cu metal adatoms forms unidentate Cu–carboxylate bonds with adjacent TMA molecules (Figure 2d). The dimer binds to the surface by 6.3 eV with respect to isolated Cu atoms, and each adatom is fivefold coordinated to the substrate. This structure has the correct 5× periodicity. Its simulated STM image (Figure 2e) closely agrees with that found experimentally, with the Cu–Cu dimer imaged as a single spot centered between the adatoms. The resulting Cu–O distance is 2.02 Å, which lies in the range of typical Cu–O bond lengths. Also the calculated apparent heights, 170 pm for the TMA unit and 90 pm for the Cu adatom unit, are in good agreement with those determined experimentally.

The theoretical analysis provides an unprecedented level of insight into the adsorption geometry of surface MOCNs. The phenyl ring of TMA and the Cu adatoms are located on the short-bridge and hollow sites, respectively (Figure 2d). The molecule stands 1.14 Å above the outermost Cu layer, with the carboxylate groups bending towards the surface by as much as 0.69 Å. With respect to a neutral Cu atom, surface complexation of Cu weakly reduces the metal center occupations of both the s and d electronic states by approximately 0.2 electrons.

[-Cu-TMA-Cu-]$_n$ chains are the intrinsic nanostructures on Cu(110), but functional MOCCs also require different elements than Cu as metallic centers. Extrinsic [-TMA-Fe-]$_n$ chains (MOCC-II) were created by holding the Cu(110) crystal at 230 K—thus preventing the formation of Cu–TMA complexes—and by depositing first TMA and then Fe at coverages higher than 0.04 ML. The sample was then annealed to 390 K for one minute. The number of chains increased with the amount of deposited Fe and saturation was reached for a coverage of around 0.08 ML of Fe. Further deposition of Fe results in the nucleation of Fe islands.

The 4× in-chain periodicity of these chains (Figure 3) leaves space for just one Fe metal center between TMA molecules. The TMA–TMA distances are therefore shorter when linked by Fe than when linked by Cu, similar to that reported for 2D MOCNs on the Cu(001) surface.[9,10] According to DFT calculations the geometry of the adsorbed TMA molecule is weakly dependent on the metal center, with the phenyl ring lying 0.09 Å higher in the case of Fe. The metal–carboxylate bond is still unidentate and the Fe–O distance is 1.95 Å, thus 0.07 Å shorter than the Cu–O distance in

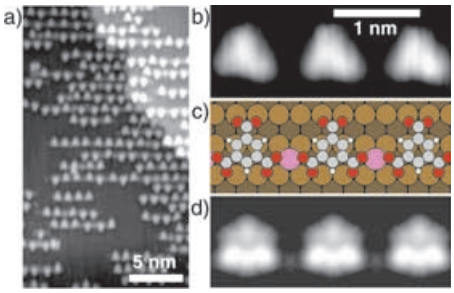

Figure 3. [-TMA-Fe-]$_n$ chains (MOCC-II): a) Overview image of the coordination chains formed upon deposition of 0.04 ML Fe and 0.40 ML TMA. Comparison of b) the high-resolution STM image, c) the atomistic MOCC-II model, and d) the corresponding simulated STM image.

MOCC-I. Single metal centers lead to very weak features in the simulated STM image (Figure 3d), in agreement with experiment (Figure 3b). With respect to a neutral Fe atom, surface complexation of Fe strongly reduces the occupations of the Fe s states by 1.3 electrons while it increases that of the d states by 0.5 electrons.

Insight into the potentially interesting magnetic properties of Fe-complexed MOCC-II can be gained by projecting the electron density on the atomic Fe d orbitals (Figure 4b).

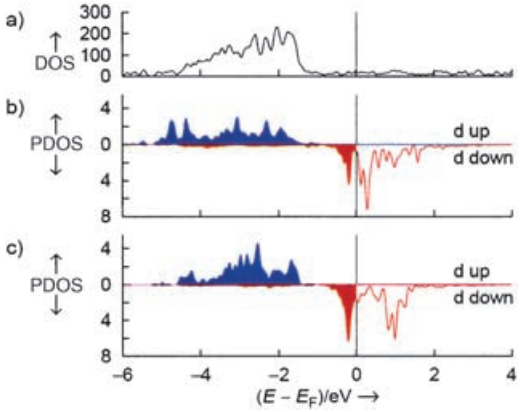

Figure 4. a) Total density of electronic states (DOS, in [eV] with respect to the Fermi energy E_F) of the [-TMA-Fe-]$_n$ chain (MOCC-II). Projected DOS (PDOS) on the atomic d states of b) the Fe center in MOCC-II and c) an Fe atom isolated on the Cu(110) surface.

The projected density of electronic states (DOS) displays a large splitting between the majority spin-up and minority spin-down electronic d states. The former are completely filled and well hybridized with the substrate Cu d states, extending from −5 to −1 eV in the total DOS of the [-TMA-Fe-]$_n$ chain (Figure 4a). The latter spin-down states are only partially filled and extend in the energy region dominated by the substrate s states. As a consequence, the Fe atoms are strongly magnetized with a spin polarization of 3.3 μ_B per Fe atom. The polarization of a Fe adatom isolated on the Cu(110) surface is very similar, 3.2 μ_B, and the corresponding projected DOS is shown in Figure 4c. The comparison shows that the coordination with the carboxylate group does not affect the electron localization at the Fe adatoms and thus

does not produce any relevant quenching of the spin magnetic moment. This is a necessary (although not sufficient) condition for the emergence of intriguing magnetic properties induced by the low dimensionality, such as a giant magnetic anisotropy.[28,29] Because of their high thermal stability, MOCNs similar to those presented here could thus be convenient model systems to explore the occurrence of low-dimensional magnetism.

In conclusion, metal–organic coordination chains were created in situ by self-organized growth at a metal surface under UHV. The 1D anisotropy of the substrate was effectively transferred to the resulting metal–organic coordination chains. This strategy was shown to work for intrinsic as well as for extrinsic metal–carboxylate systems. The precise atomic configuration of the structures was revealed by a combined use of STM and DFT. Spin-polarized DFT suggests that Fe centers within the 1D chains have magnetic properties similar to those of isolated Fe adatoms. This renders such regular and unidirectional arrangement of magnetic centers attractive candidates for the investigation of low-dimensional magnetism in thermally stable structures.

Experimental Section

Methods: The sample was prepared in a standard UHV preparation chamber with a base pressure of less than 2×10^{-10} mbar. The Cu(110) single crystal was cleaned by cycles of Ar^+ sputtering (900 eV) and annealing to 830–850 K. Commercially available TMA (Fluka Chemie AG, purity > 97%) was evaporated from a ceramic crucible at 460 K for sample temperatures between 130 K and 300 K. The sample was then transferred under UHV conditions to a STM chamber (base pressure of 6×10^{-11} mbar) that comprised a commercial variable-temperature STM apparatus. Measurements were carried out at 300 K and 130 K with typical tunneling conditions of −1 V and 1 nA (filled-state imaging).

The computer simulations were based on DFT, in the generalized gradient approximation of Perdew–Burke–Ernzerhof.[30] The calculations were performed in the pseudopotential plane-wave framework (plane-wave cutoff of 326.4 eV) using ultrasoft pseudopotentials[31] as implemented in the PWscf simulation package.[32] A three-layer slab provided a simplified model of the Cu(110) surface. The atomic positions were determined by relaxing the upper layer and keeping the distance between the others fixed at the bulk value. Metal adatoms and deprotonated TMA molecules were positioned on the upper surface of the slab and were structurally relaxed according to the Hellmann–Feynman forces. STM images were simulated by means of the Tersoff–Hamann method,[33] that is, by a spatially resolved DOS integrated in energy from a bias potential (−1.0 eV) to the Fermi energy.

Received: June 10, 2005

Keywords: coordination modes · density functional calculations · nanostructures · scanning probe microscopy · self-assembly

[1] O. M. Yaghi, M. O'Keeffe, N. W. Ockwig, H. K. Chae, M. Eddaoudi, J. Kim, *Nature* **2003**, *423*, 705.
[2] G. F. Swiegers, T. J. Malefetse, *Chem. Rev.* **2000**, *100*, 3483.
[3] B. J. Holliday, C. A. Mirkin, *Angew. Chem.* **2001**, *113*, 2076; *Angew. Chem. Int. Ed.* **2001**, *40*, 2022.
[4] C. Copéret, M. Chabanas, R. P. Saint-Arroman, J.-M. Basset, *Angew. Chem.* **2003**, *115*, 164; *Angew. Chem. Int. Ed.* **2003**, *42*, 156.
[5] C. Nozaki, C. G. Lugmair, A. T. Bell, T. Don Tilley, *J. Am. Chem. Soc.* **2002**, *124*, 13194.
[6] H. Srikanth, R. Hajndl, B. Moulton, M. J. Zaworotko, *J. Appl. Phys.* **2003**, *93*, 7089.
[7] A. Dmitriev, H. Spillmann, N. Lin, J. V. Barth, K. Kern, *Angew. Chem.* **2003**, *115*, 2774; *Angew. Chem. Int. Ed.* **2003**, *42*, 2670; S. Stepanow, M. Lingenfelder, A. Dmitriev, H. Spillmann, E. Delvigne, N. Lin, X. Deng, C. Cai, J. V. Barth, K. Kern, *Nat. Mater.* **2004**, *3*, 229.
[8] D. G. Kurth, N. Severin, J. P. Rabe, *Angew. Chem.* **2002**, *114*, 3833; *Angew. Chem. Int. Ed.* **2002**, *41*, 3681.
[9] N. Lin, A. Dmitriev, J. Weckesser, J. V. Barth, K. Kern, *Angew. Chem.* **2002**, *114*, 4973; *Angew. Chem. Int. Ed.* **2002**, *41*, 4779.
[10] P. Messina, A. Dmitriev, N. Lin, H. Spillmann, M. Abel, J. V. Barth, K. Kern, *J. Am. Chem. Soc.* **2002**, *124*, 14000.
[11] S. De Feyter, M. M. S. Abdel-Mottaleb, N. Schuurmans, B. J. V. Verkuijl, J. H. van Esch, B. L. Feringa, F. C. De Schryver, *Chem. Eur. J.* **2004**, *10*, 1124.
[12] M. Ruben, *Angew. Chem.* **2005**, *117*, 1620; *Angew. Chem. Int. Ed.* **2005**, *44*, 1594.
[13] J.-M. Lehn, *Supramolecular Chemistry*, VCH, Weinheim, **1995**, chap. 9, p. 200.
[14] M. Ruben, J. Rojo, F. J. Romero-Salguero, L. H. Uppadine, J.-M. Lehn, *Angew. Chem.* **2004**, *116*, 3728; *Angew. Chem. Int. Ed.* **2004**, *43*, 3644.
[15] H. Röder, E. Hahn, H. Brune, J.-P. Bucher, K. Kern, *Nature* **1993**, *366*, 141.
[16] S. Lukas, G. Witte, C. Wöll, *Phys. Rev. Lett.* **2002**, *88*, 028301.
[17] A. Kühnle, L. M. Molina, T. R. Linderoth, B. Hammer, F. Besenbacher, *Phys. Rev. Lett.* **2004**, *93*, 086101.
[18] P. Gambardella, M. Blanc, H. Brune, K. Kuhnke, K. Kern, *Phys. Rev. B* **2000**, *61*, 2254.
[19] P. W. Murray, I. M. Brookes, S. A. Haycock, G. Thornton, *Phys. Rev. Lett.* **1998**, *80*, 988.
[20] S. Griessl, M. Lackinger, M. Edelwirth, M. Hietschold, W. M. Heckl, *Single Mol.* **2002**, *3*, 25.
[21] Y. Ishikawa, A. Ohira, M. Sakata, C. Hirayama, M. Kunitake, *Chem. Commun.* **2002**, *22*, 2652.
[22] G.-J. Su, H.-M. Zhang, L.-J. Wan, C.-L. Bai, T. Wandlowski, *J. Phys. Chem. B* **2004**, *108*, 1931.
[23] C. C. Perry, S. Haq, B. G. Frederick, N. V. Richardson, *Surf. Sci.* **1998**, *409*, 512.
[24] N. Lin, D. Payer, A. Dmitriev, T. Strunskus, C. Wöll, J. V. Barth, K. Kern, *Angew. Chem.* **2005**, *117*, 1512; *Angew. Chem. Int. Ed.* **2005**, *44*, 1488.
[25] S. Stepanow, T. Strunskus, M. Lingenfelder, A. Dmitriev, H. Spillmann, N. Lin, J. V. Barth, C. Wöll, K. Kern, *J. Phys. Chem. B* **2004**, *108*, 19392.
[26] D. S. Martin, R. J. Cole, S. Haq, *Phys. Rev. B* **2002**, *66*, 155427.
[27] A. Doyle, J. Felcman, M. T. do Prado Gambardella, C. N. Verani, M. L. Bragança Tristão, *Polyhedron* **2000**, *19*, 2621.
[28] P. Gambardella, A. Dallmeyer, K. Maiti, M. C. Malagoli, W. Eberhardt, K. Kern, C. Carbone, *Nature* **2002**, *416*, 301.
[29] P. Gambardella, S. Rusponi, M. Veronese, S. S. Dhesi, C. Grazioli, A. Dallmeyer, I. Cabria, R. Zeller, P. H. Dederichs, K. Kern, C. Carbone, H. Brune, *Science* **2003**, *300*, 1130.
[30] J. P. Perdew, K. Burke, M. Ernzerhof, *Phys. Rev. Lett.* **1996**, *77*, 3865.
[31] D. Vanderbilt, *Phys. Rev. B* **1990**, *41*, 7892.
[32] S. Baroni, A. Dal Corso, S. de Gironcoli, P. Giannozzi, http://www.pwscf.org.
[33] J. Tersoff, D. R. Hamann, *Phys. Rev. Lett.* **1983**, *50*, 1998.

